Control Engineering Practice 21 (2013) 122–133

Contents lists available at SciVerse ScienceDirect

Control Engineering Practice

journal homepage: www.elsevier.com/locate/conengprac

Practical adaptive filter controls for precision beam pointing and tracking with jitter attenuation

Michael J. Beerer [a,1], Hyungjoo Yoon [a,b,2,*], Brij N. Agrawal [a,3]

[a] U.S. Naval Postgraduate School, Monterey, CA 93943, USA
[b] Korea Aerospace Research Institute, 169-84 Gwahangno, Yuseong, Daejeon 305-806, Republic of Korea

ARTICLE INFO

Article history:
Received 10 November 2011
Accepted 30 September 2012
Available online 23 October 2012

Keywords:
Adaptive filter
Laser beam pointing
Jitter control
Target tracking
Least mean squares (LMS) filter
Recursive least squares (RLS) filter

ABSTRACT

The imaging, pointing, and tracking performance of precision optical systems are degraded by various disturbances which induce optical beam jitter. The present research proposes adaptive filter control methods for actively attenuating beam jitter using a fast steering mirror. Control loops with various structures of adaptive transversal filters are developed to suppress time-varying or uncertain jitter, and their characteristics and performances are compared. In particular, for situations when obtaining reference signals which are fully coherent with the disturbance is not possible, methods for incorporating multiple semi-coherent reference signals into the control law are developed. An index variable is defined to measure quality of various references signals, and a few signals are selected based on this index. The developed controllers are verified on a jitter control testbed, and experimental results show that the adaptive methods show superior performance in jitter attenuation over the conventional non-adaptive method.

1. Introduction

Optical beam jitter control has become a topic of great interest with various applications in directed energy weapons, free-space laser communications, precision laser machining, adaptive optics, etc. The objective of this research is to use a fast steering mirror to point a laser beam accurately at a target in the presence of jitter. Jitter is defined as mixture of pitch and yaw motions of an optical beam away from line of sight, which are caused by various disturbances. It is generally an angular quantity (measured in radians), but the errors are manifested when the beam strikes some two-dimensional surface, such as a position sensing detector (PSD) or a CCD array, and is then measured as a distance or number of pixels (Anderson, Blankinship, Fowler, Glaese, & Janzen, 2007). The disturbances include mechanical vibrations on the optical platform and jitter induced by atmospheric turbulence, and they may have time varying spectrum or unknown characteristics. Mechanical vibrations caused by rotary or repetitive devices (engines, actuators, electric motors, etc.) onboard the platform induce narrowband jitter. Atmospheric induced jitter is spread over a wide range of frequencies causing broadband (or random) jitter. A method for attenuating these jitters must be developed in order to allow high precision optical devices to operate.

Many methods to control optical beam jitter have been proposed in the literature (Anderson et al., 2007; Bateman, 2007; McEver, Cole, & Clark, 2004; Orzechowski, Gibson, & Tsao, 2004, 2006; Pérez Arancibia, Chen N. Y., Gibson, & Tsao, 2006; Pérez Arancibia, Chen N., Gibson, & Tsao, 2006; Watkins, 2004; Watkins & Agrawal, 2007; Yoon, Bateman, & Agrawal, 2008, 2011). These methods can be categorized into two types: *feedback control*, where the controller reduces the jitter using only the error signal (the difference between the desired and actual beam positions) at the target, and *feedforward control*, where the controller uses a reference signal, which is highly correlated with the disturbance source.

The conventional linear-time-invariant (LTI) feedback control techniques such as proportional-integral-derivative (PID) control and linear-quadratic-Gaussian (LQG) control are most commonly used in practical applications, but they may have difficulty handling the non-stationary disturbances with time-varying nature. Gibson, Tsao, and their research team have published a series of papers (Orzechowski et al., 2004, 2006; Pérez Arancibia, Chen N. Y., et al., 2006; Pérez Arancibia, Chen N., et al., 2006), on beam jitter control using a feedback recursive least-squares (RLS) lattice filter algorithm, which was originally developed in Jiang and

* Corresponding author at: Korea Aerospace Research Institute, 169-84 Gwahangno, Yuseong, Daejeon 305-806, Republic of Korea. Tel.: +82 10 3324 3660; fax: +82 42 860 2898.
E-mail addresses: mbeerer@gmail.com (M.J. Beerer), drake.yoon@gmail.com (H. Yoon), agrawal@nps.edu (B.N. Agrawal).
URL: http://www.drake.googlepages.com (H. Yoon).
[1] U.S. Air Force Civilian.
[2] Satellite Control System Department.
[3] Department of Mechanical and Astronautical Engineering, Director of Space Research and Design Center.

0967-0661/$ - see front matter © 2012 Elsevier Ltd. All rights reserved.
http://dx.doi.org/10.1016/j.conengprac.2012.09.018

Gibson (1995). Their scheme shows significant jitter rejection but the lattice filter algorithm is so complicated that it is not easy to implement it in a practical system without thorough understanding of it. McEver et al. (2004) also proposed adaptive feedback control using the Q-parameterization method.

Adaptive feedforward control may be used when a reference signal, which is highly correlated with the disturbances, is available in real time. The reference signal is fed into a transversal filter whose filter gains, or weights, are updated using the error signal. Inspired by adaptive filter methods used in active noise control (Kuo & Morgan, 1996; Watkins, 2004; Watkins & Agrawal, 2007) proposed the use of filtered-x least mean squares (FX-LMS) adaptive feedforward controller in the beam jitter rejection. Bateman (2007) and Yoon et al. (2008, 2011) also proposed adaptive filter methods adopting filtered-x recursive least squares (FX-RLS) algorithm.

The disadvantage of any adaptive feedforward algorithm is that they require reference signals (Kuo & Morgan, 1996). For good jitter rejection, the reference signal must be correlated with the entire frequency content of the disturbances which are made up from various sources. For instance, Watkins (2004), Watkins and Agrawal (2007), Yoon et al. (2008, 2011), and Bateman (2007) use a sensor which is installed to generate such reference signals. However, such reference signals may be unavailable in real applications. Even in such a case, it may be still possible to implement adaptive feedforward control by fusing together information from multiple semi-coherent reference signals that are only correlated with some component of the total disturbance. In these situations, the simple conventional adaptive methods would not effectively attenuate the disturbances, and thus other adaptive methods that utilize multiple reference signals should be employed for better jitter rejection.

In this paper, the FX-LMS and FX-RLS methods developed in Watkins (2004), Watkins and Agrawal (2007), Yoon et al. (2008, 2011) and Bateman (2007) are modified to use information from multiple reference signals. The multiple-channel adaptive filter techniques have been presented in active noise control applications, but their successful use has been limited to cases involving repetitive noise with a few harmonics (Kuo & Morgan, 1996). In the present research, two methods for combining the multiple reference signals in the control law are developed. These modifications give the adaptive feedforward control technique more functionality in applications where a fully coherent reference signal is not available.

In addition, feedback adaptive filter methods that do not require measurement of any reference signal are developed. In this method, a reference signal is internally estimated using the measured output error and the filter output. A hybrid technique that combines feedback, feedforward adaptive filters and LTI controller is also proposed. With slight modification, the developed algorithms can be applied not only to stationary target pointing but also to dynamic target tracking. If the target dynamics is fast relative to the filter adaptation speed, the adaptive-only methods cannot track the moving target. It will be shown that the hybrid method which combines the adaptive and LTI control methods can successfully achieve this control objective.

An experimental laser jitter control testbed, equipped with a fast steering mirror to correct the beam, has been developed to test various control techniques. Using this testbed, the developed jitter control algorithms are experimentally validated and compared.

2. Experimental setup

The jitter control testbed at the Spacecraft Research and Design Center, U.S. Naval Postgraduate School, Monterey, CA, USA was used for this experiment. Figs. 1 and 2 show the schematic and the picture of the testbed, respectively.

The testbed contains a laser source, 3-axis accelerometer, beam splitter, two inertial actuators (shakers), two position sensing detectors (PSD, referred to as PD-1 and PD-2), and two fast steering mirrors (referred to as a control fast steering mirror

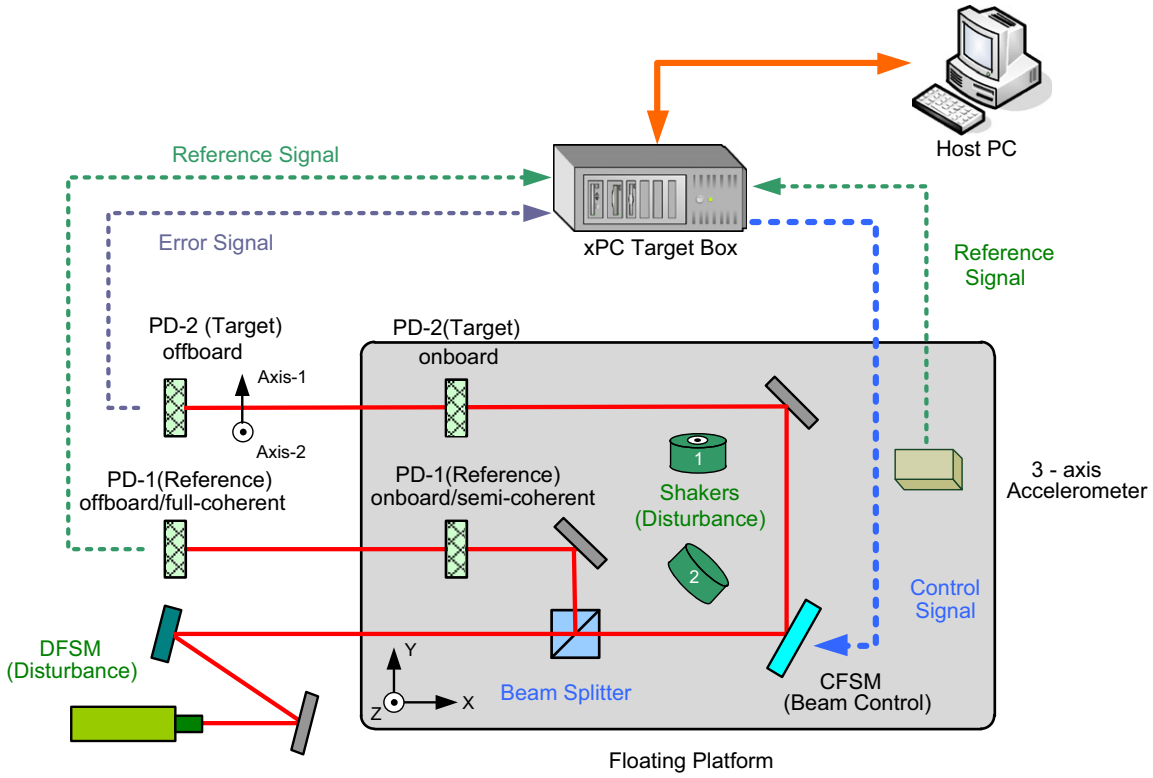

Fig. 1. Diagram of the testbed. PD-1 and PD-2 are shown in both their on-board and off-board positions.

(CFSM) and a disturbance fast steering mirror (DFSM)). As shown in Figs. 1 and 2 some of these components are mounted on a floating platform of which its original purpose is to isolate the components from external vibrations, but in this research it is used to simulate a spacecraft/aircraft's vibrational environment. Two shakers are mounted orthogonally to one another on the platform to create narrowband vibrations along different axes of the platform: Shaker 1 is mounted along the *Z*-axis of the table so that it creates vibration primarily along the *Z*-axis, and Shaker 2 is mounted horizontally to the platform in order to provide vibrations along the *X*- and *Y*-axes. All the optics on-board the vibration platform are subjected to the shaker disturbances. A 3-axis accelerometer is mounted near the shakers to provide signals correlated with the shaker disturbances.

The laser propagates from the source to the DFSM where it is given a broadband (random) disturbance to simulate the effects of atmospheric turbulence. The beam passes onto the vibration platform and is split into two beams by the beam splitter. One beam passes through the splitter and propagates to the CFSM where control inputs are applied to the beam from the control computer. The beam then propagates to the target PSD (PD-2) which is providing an error signal to the control computer. In order to simulate various beam control scenarios, the target sensor (PD-2) can be mounted both on-board or off-board the vibration platform during the experiments. With the target sensor off-board the platform, the testbed simulates scenarios in which the optical system needs to direct a laser beam to a far away target, such as a free-space laser communications transmitter, an optical relay spacecraft, or airborne/spaceborne laser weapon systems. When the target sensor is located on-board the platform, the testbed simulates a scenario such as a free-space laser communications receiver, or a jitter control system in a laser resonator. The present paper mainly investigates cases of the off-board target, but the developed schemes can be easily applied for the on-board target case.

The other beam split by the beam splitter is redirected onto the reference signal PSD (PD-1). When the position sensor PD-1 is mounted off the vibration platform, as in Watkins (2004), Watkins and Agrawal (2007), Yoon et al. (2008, 2011) and Bateman (2007), it provides a fully coherent reference signal that is highly correlated with both the disturbances from the DFSM and the shakers. This configuration may reflect ground-based applications, like an astronomical telescope, but may not reflect spacecraft/aircraft applications. When PD-1 is mounted on the vibration platform and subjected to the shaker disturbance, it continues to provide a signal correlated with the DFSM disturbance. In this configuration, however, its correlation with the shaker disturbances is degraded. In this paper, the on-board PD-1 signal along with an accelerometer signal (correlated with the shaker disturbances) will be used, and the results are compared to the off-board PD-1 reference signal experiments. In addition, a feedback adaptive filter that internally generates a reference signal instead of using the measured reference signals will be tested. The degree of correlation between the various reference signals and the disturbances is summarized later in the paper.

The beam positions at the PSDs are reported in the Axis-1 and Axis-2 coordinate system while the accelerometer signals are reported in the *X*, *Y* and *Z* coordinates, both are shown in Fig. 1. Beerer (2008) contains a more detailed description of the testbed, while Table 1 provides the product name and company of the equipments.

The control law is designed in MATLAB Simulink with Real-Time Workshop and xPC Target toolbox. The control law is compiled and downloaded to an xPC target PC with an Intel quad-core 2.66 GHz processor. A sample rate of 2 kHz is used throughout the experiment. Cross-coupling between the two axes

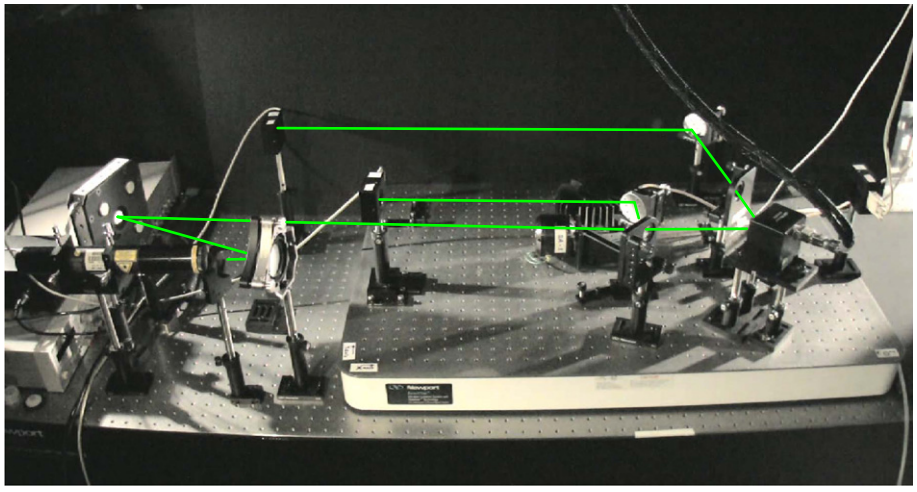

Fig. 2. Jitter control testbed. PD-1 shown in on-board position, PD-2 shown in off-board position.

Table 1
List of equipments used in the testbed.

Equipment	Manufacturer	Model
PSD	On-Trak	PSM2-10 (with OT-301 amplifier)
CFSM	Newport	FSM200 (with FSM-CD-100 controller box)
DFSM	Baker adaptive optics	Light force one
Shaker 1	Aura	AST-2B-4 Pro Bass shaker
Shaker 2	CSA engineering	SA-5 inertial actuator
Accelerometer	Kistler	8690C10 3-axis accelerometer (with 5124A Piezotron Coupler)
Floating platform	Newport	BT-2436 bench top

of the CFSM has been shown previously to be negligible by experiments (Watkins, 2004). Therefore, it is assumed that they have zero coupling, and the control laws are applied independently between the two axes of the mirror.

3. Feedforward adaptive filters: review

There are several different structures in adaptive filters that may be used for beam jitter control, and the simplest transversal filter is the choice of this paper. Here the fundamental of the adaptive transversal filter theory is reviewed, which will be modified in the later part of the paper.

In an adaptive transversal filter, a reference signal is input to the transversal filter, consisting of $M-1$ unit-delay elements and M tap weights. The number of tap weights, M, is commonly referred to as the filter length. (The number of delay elements, $M-1$, is referred to as the filter order.) The error between the desired beam location at the target and the actual location, $e(n)$, is fed back to the filter to adjust these weights. The output of the transversal filter is the control signal to the CFSM, $y(n)$.

The reference signal, $r(n)$, is delayed one time step for each of the $M-1$ delay elements, forming a vector of delayed inputs, $\mathbf{r}(n)=[r(n),r(n-1),\ldots,r(n-M+1)]^T\in R^M$. The inner product of the vector of weights $\mathbf{w}(n)=[w_1(n),w_2(n),\ldots,w_M(n)]^T\in R^M$ and the vector of reference signal inputs, $\mathbf{r}(n)$, produces the scalar output $y(n)$:

$$y(n)=\mathbf{w}^T(n)\mathbf{r}(n) \tag{1}$$

Therefore, the error signal at the position sensor is

$$e(n)=d(n)-s(n)*y(n) \tag{2}$$

where $d(n)$ is the disturbance, $*$ denotes linear convolution, and $s(n)$ is the impulse response of the *secondary plant dynamics* $S(z)$ from the filter output $y(n)$ through CFSM to target sensor (PD-2) output. (The *primary plant* is the path from the disturbance source to the error at the target.)

The goal of the adaptive updating algorithm is to adaptively update the weighting vector to minimize the error signal, usually represented as the mean square error, $\xi=E[e^2(n)]$, where $E[\cdot]$ denotes the statistical expectation operator. The conventional, or 'bare-bone', adaptive filtering algorithms in textbooks are developed with neglect of the secondary plant dynamics $S(z)$, i.e., $e(n)=d(n)-\mathbf{w}^T(n)\mathbf{r}(n)$. However, in this study, the output from the controller, $y(n)$, must pass through the secondary plant $S(z)$ which causes shifts in gain and phase. Using an assumption that $S(z)$ and the transversal filters are commutable, the error signal in Eq. (2) can be written as

$$e(n)=d(n)-\mathbf{w}^T(n)\hat{\mathbf{r}}(n) \tag{3}$$

where the vector $\hat{\mathbf{r}}(n)$ is constructed using a filtered reference signal $\hat{r}(n)$ such that

$$\hat{r}(n)=\hat{s}(n)*r(n) \tag{4}$$

where $\hat{s}(n)$ is the impulse response of $\hat{S}(z)$ which is a copy of $S(z)$ and needs to be modeled or identified for implementation. Then using a filtered reference signal $\hat{\mathbf{r}}(n)$, one can utilize conventional adaptive filter algorithms (which were developed with neglect of $S(z)$) in updating the weighting parameters. This method has been widely used in some applications (for instance, active noise control) and is referred to as the Filtered-X method in the literature (Kuo & Morgan, 1996). Fig. 3 shows the feedforward Filtered-X method implemented in the controller. Hereafter, for simplicity, $r(n)$ is used to denote the filtered reference signal.

3.1. Wiener filter: linear optimal solution

The Wiener filter is the optimum linear discrete time filter for estimating the disturbance. It is a non-adaptive method and requires an assumption that the disturbance is both stationary and the spectral properties are known. The Wiener filter is not practical for jitter control because of the unknown and time-varying nature of the jitter. However, the Wiener filter solution can be used as a reference for the best case jitter rejection for given disturbance and reference signals by the adaptive filter methods under study. Both the LMS and RLS algorithms converge to the optimal Wiener filter weighting. Assuming that the filter input and the disturbance have zero mean (when the signals have non-zero mean, this assumption can be justified by using bias-estimating adaptive filters, Yoon et al. (2008, 2011), and/or using additional control loops in parallel), it can be shown that the minimum Wiener controlled jitter with given reference and disturbance signals is Haykin (2001):

$$\xi_{\min}=\sigma^2_{\min}=E[d^2(n)]-\mathbf{p}^{\mathrm{T}}\mathbf{R}^{-1}\mathbf{p} \tag{5}$$

where $\mathbf{R}$ is the autocorrelation matrix of the reference signal, $\mathbf{R}=E[\mathbf{r}(n)\mathbf{r}^{\mathrm{T}}(n)]$, and $\mathbf{p}$ is the cross-correlation vector between the reference signal and the disturbance, $\mathbf{p}=E[\mathbf{r}(n)d(n)]$. As a tool for comparison, the ratio between the optimal Wiener disturbance

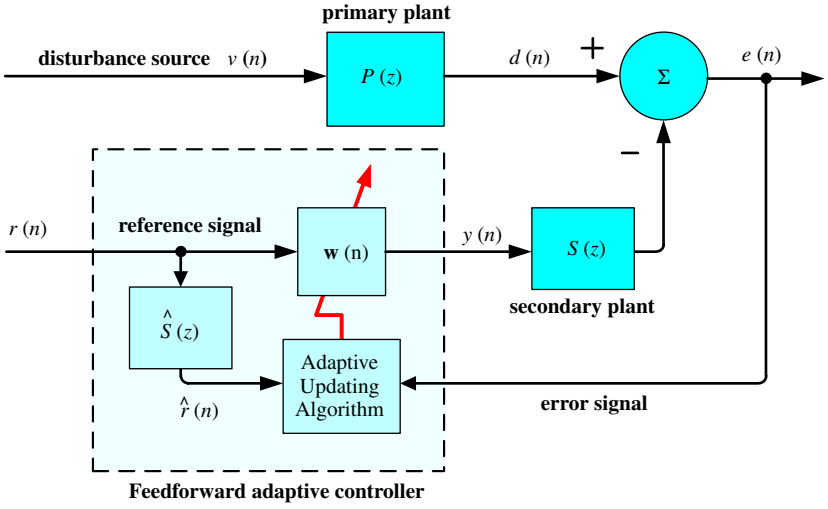

Fig. 3. Feedforward adaptive control implementation.

rejection and total disturbance is defined:

$$\gamma_{\text{opt}} = \frac{\sigma_d - \sigma_{\min}}{\sigma_d} \tag{6}$$

where σ_d is the standard deviation of the beam position at the target with jitter and without any control. Since $\xi_{\min}$ is the best rejection performance with a given reference signal, $\xi_{\min}$, or equivalently γ_{opt}, can be used as an index (or measure) of 'quality' of the reference signal. The index variable γ_{opt} has a value between 0 and 1: $\gamma_{\text{opt}} = 0$ means no disturbance attenuation can be obtained with given reference signal, and $\gamma_{\text{opt}} = 1$ means perfect attenuation can be obtained.

In order to evaluate controller performance in experiments, the ratio between the controlled disturbance rejection and the total disturbance can be similarly defined:

$$\gamma_{\text{cont}} = \frac{\sigma_d - \sigma_{\text{cont}}}{\sigma_d} \tag{7}$$

where σ_{cont} is the standard deviation of the beam position at the target with control applied.

3.2. Adaptive updating algorithms

The least-mean-squares algorithm (LMS) is one of the simplest adaptive algorithms and has become a standard for comparison with more complex algorithms. The LMS algorithm to update the weightings can be written as follows (Kuo & Morgan, 1996):

$$\mathbf{w}(n+1) = \mathbf{w}(n) - \mu \mathbf{r}(n) e(n) \tag{8}$$

where μ is the convergence factor.

The recursive-least-squares (RLS) algorithm generally provides faster convergence and smaller steady state error than the LMS algorithm (Yoon et al., 2008). The transversal filter structure of the FX-RLS algorithm is identical to that of FX-LMS, the difference is the weight updating algorithm. The RLS algorithm to update the weighting vector $\mathbf{w}(n)$ at each instance is the following (Haykin, 2001; Kuo & Morgan, 1996):

$$\mathbf{k}(n) = \frac{\lambda^{-1} Q(n-1)\mathbf{r}(n)}{1 + \lambda^{-1}\mathbf{r}^T(n) Q(n-1)\mathbf{r}(n)} \tag{9}$$

$$\mathbf{w}(n) = \mathbf{w}(n-1) + \mathbf{k}(n) e(n) \tag{10}$$

$$Q(n) = \lambda^{-1} Q(n-1) - \lambda^{-1}\mathbf{k}(n)\mathbf{r}^T(n) Q(n-1) \tag{11}$$

where λ is a forgetting factor ($0 < \lambda \leq 1$), $\mathbf{k}(n) \in R^M$ is the time-varying gain vector, and $Q(n) \in R^{M \times M}$ is the inverse correlation matrix. See Kuo and Morgan (1996) and Haykin (2001) for more details on the LMS and the RLS algorithms.

Finally, one may slightly modify the definition of the reference signal and weighting vector to take into account the presence of a DC component in the error signal. This method is referred to as bias estimation (Yoon et al., 2008, 2011) and requires the addition of a constant element to the reference signal vector and a corresponding weight to track the bias:

$$\mathbf{r}_b^T(n) = [1,\ \mathbf{r}^T(n)] = [1,\ r(n),\ r(n-1), \ldots, r(n-M+1)]^T \in R^{M+1} \tag{12}$$

$$\mathbf{w}_b^T(n) = [w_b(n),\ \mathbf{w}^T(n)] = [w_b(n),\ w_1(n),\ w_2(n), \ldots, w_M(n)]^T \in R^{M+1} \tag{13}$$

Notice that the reference signals in the adaptive updating algorithms should be filtered by the secondary plant model for the Filtered-X method.

4. Feedforward adaptive filters with multiple reference signals

In Watkins (2004), Watkins and Agrawal (2007), Yoon et al. (2008, 2011) and Bateman (2007), the FX-LMS and FX-RLS algorithms described above have a standard transversal filter structure which use a single-channel reference signal for control in each axis of PD-2 off-board the platform. In the present paper, two reference signals that are each correlated with only a component of the total beam jitter are provided. Now two methods will be developed for implementing the controllers with multiple reference signals. The reference signals are provided by the on-board accelerometer and the on-board PSD (PD-1). When using two reference signals, a distinction is given between the number of accelerometer taps (denoted as M_a) and PSD taps (denoted as M_p).

4.1. Method 1: summation of filter outputs

As described in Fig. 4, Method 1 uses two separate control blocks (an accelerometer block and a PSD block). The individual outputs are summed and sent to the CFSM. This method is easy to implement because one does not need to modify the standard adaptive filter loops. In addition, when using the RLS algorithm, it will manipulate two inverse correlation matrices per axis: $Q_{Accel}(n) \in R^{(M_a+1)\times(M_a+1)}$ and $Q_{PSD}(n) \in R^{(M_p+1)\times(M_p+1)}$. The standard RLS algorithm requires on the order of M^2 (i.e., $\mathcal{O}\{(M^2)\}$) operations per time step (Kuo & Morgan, 1996). As a result, Method 1 requires a total of $\mathcal{O}\{(M_a+1)^2+(M_p+1)^2\}$ (or $\mathcal{O}\{(M_a)^2+(M_p)^2\}$ without the bias estimators) operations, which is of lower order than that of the second method presented in the next section. On the other hand, because placing the adaptive filters in parallel may cause unexpected interactions, their performance and characteristics may not be easy to predict or

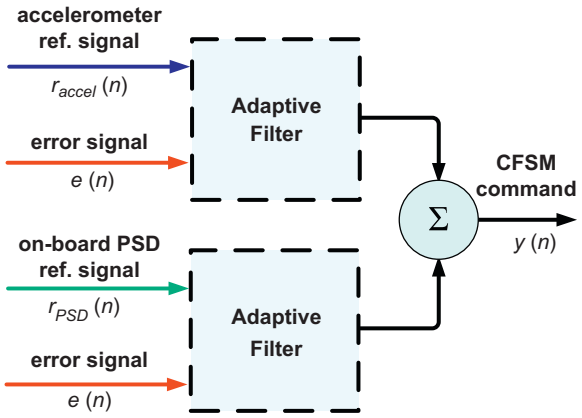

Fig. 4. Adaptive filters with multiple reference signals using Method 1.

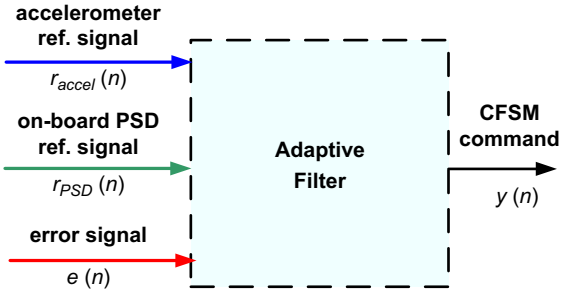

Fig. 5. Adaptive filter with multiple reference signals using Method 2.

analyze mathematically as opposed to an individual adaptive filter.

4.2. Method 2: augmentation of reference signals

As described in Fig. 5 for Method 2, the reference signals are combined inside a single control block. The reference signal and weight vectors are modified to contain both accelerometer and PSD taps:

$$\mathbf{r}(n) = [1,\ r_{Accel}(n),\ r_{Accel}(n-1), \ldots, r_{Accel}(n-M_a+1), \\ r_{PSD}(n),\ r_{PSD}(n-1), \ldots, r_{PSD}(n-M_p+1)]^T \quad (14)$$

$$\mathbf{w}(n) = [w_b(n),\ w_1(n),\ w_2(n), \ldots, w_{M_a+M_p}(n)]^T \quad (15)$$

where $r_{Accel}(n)$ and $r_{PSD}(n)$ are measured reference signals from the accelerometer and the reference PSD (PD-1), respectively. (For simplicity, it is assumed that only one-axial signal out of the three-dimensional accelerometer signal is used.) The rest of the algorithm is implemented as described in Section 3.2. Method 2 has a simpler structure compared to Method 1 because it only requires one adaptive filter (for each axis). The RLS algorithm will manipulate one larger inverse correlation matrix per axis: $Q(n) \in R^{(M_a+M_p+1)\times(M_a+M_p+1)}$ and requires $\mathcal{O}\{(M_a+M_p+1)^2\}$ operations per time step. Method 2 is therefore computationally more expensive than Method 1 when the RLS algorithm with a high order filter is used. It is also noteworthy that Methods 1 and 2 are also applicable with the LMS algorithm, but computational burden is not an issue because the LMS algorithm is order of $\mathcal{O}\{M\}$.

5. Feedback adaptive filter controls

Feedback adaptive filters use the same single channel transversal filter structure as the feedforward adaptive filter controllers, but instead of using the measured reference signals, it internally generates its own reference signal using the adaptive filter output, $y(n)$, and the error signal, $e(n)$. As used in Orzechowski et al. (2004, 2006), Pérez Arancibia, Chen N. Y., et al. (2006); Pérez Arancibia, Chen N., et al. (2006), the disturbance can be estimated from Eq. (2) by

$$\hat{d}(n) = e(n) + \hat{s}(n) * y(n) \quad (16)$$

Fig. 6 shows the feedback adaptive control implementation. Comparing the feedforward and feedback algorithms in Figs. 3 and 6, respectively, shows their near identical structure. The filter output, $y(n)$, is filtered by the secondary plant estimate and then added to the error signal, $e(n)$. The secondary plant estimate, $\hat{S}(z)$, is the same that is employed for the Filtered-X method. The generated reference signal, $r(n)$, is an estimate of the primary noise signal, $d(n)$, from Eq. (2), and therefore, given the disturbance $\hat{d}(n)$. It can be shown that under ideal conditions, when $\hat{S}(z) = S(z)$, the feedback method is transformed into the feedforward method which uses the disturbance itself as a reference signal, and thus one can obtain good jitter rejection. Therefore, the performance of the feedback controller compared to the feedforward controller highly depends on obtaining an accurate secondary plant model. The feedback controller uses the same Filtered-X method and bias estimator as described in the previous sections.

5.1. Parallel PI controller

Initial testing with the feedback controller consisting only of an adaptive filter showed instability when the DC component of the error signal was large. In other words, when the beam was given a large initial bias error in addition to the DFSM and shaker disturbances, the feedback controller would behave erratically. The internal bias estimator in the adaptive filter seemed to not work as anticipated. However, when the bias error was small, the feedback controller behaved as expected.

It is thought to be due to a large initial transition of the estimated reference signal at the moment when the controller is switched on. The reference signal in a feedforward controller does not change much even as control input starts to be applied because the reference sensor is upstream of the control actuator. Experiments with a downstream feedforward reference sensor gave similar results to the feedback instability seen here. The downstream reference signal

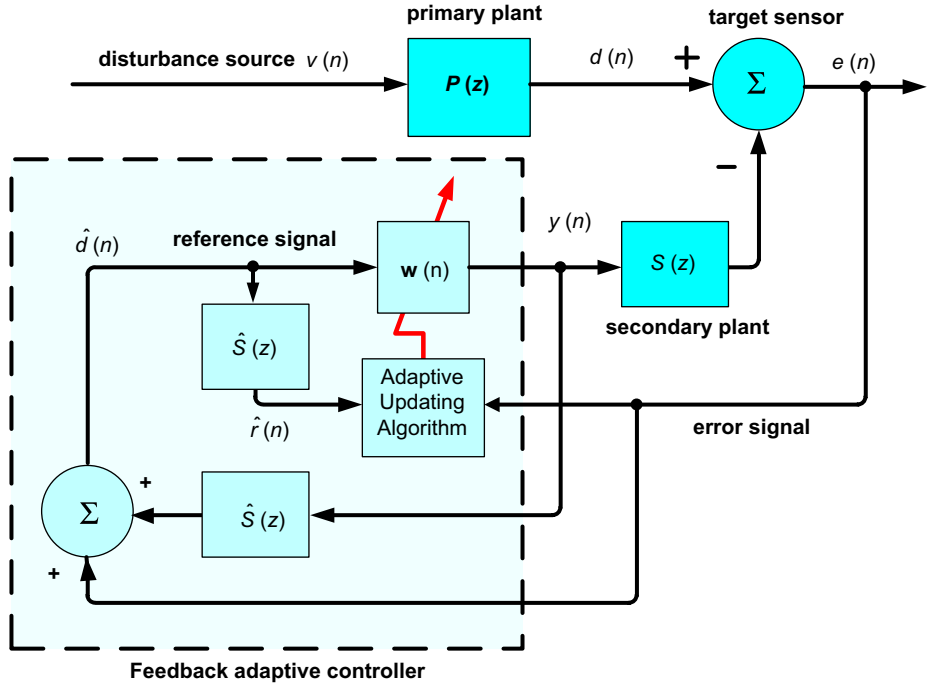

Fig. 6. Feedback adaptive control implementation.

contained a large change in the DC component when the controller was turned on due to the initial bias error being corrected. This appeared to initiate instability in the system. Inspection of the estimated feedback reference, from Eq. (16), reveals that a large initial transition is expected because the reference signal is derived from the downstream error (target) sensor.

As a solution to improve the robustness of the control method to allow for large DC biases, a proportional-integral (PI) controller was placed in parallel with the adaptive filter. An error PI controller applies fixed gains (K_p and K_i) to the error signal and the integral of the error signal as shown in

$$y_{pi}(n) = K_p \cdot e(n) + K_i \cdot T_s \sum_{k=0}^{n} e(k) \tag{17}$$

where T_s is the sampling time of the control loop. This is a classical linear time-invariant control technique which works to push the error signal towards zero. With the PI controller placed in parallel with the adaptive filter, as shown in Fig. 7, it removes the initial bias error so that feedback adaptive filter may perform correctly.

5.2. Hybrid adaptive filter

A combination of the feedback and feedforward methods is refereed to in the literature as a hybrid adaptive filter (Kuo & Morgan, 1996). In such a system, the canceling signal, $y(n)$, is generated from both a reference sensor (or sensors) and the error sensor. To accomplish this, feedback and feedforward adaptive filters are simply placed in parallel as in Kuo and Morgan (1996). This method uses both the measured reference signal(s) and the internally generated reference signal. For the same reasons mentioned in the previous section, a PI controller was placed in parallel with the hybrid controller. The hybrid controller uses parallel adaptive filters, and therefore, as mentioned earlier, is not easy to analyze mathematically. But as shown in the next section,

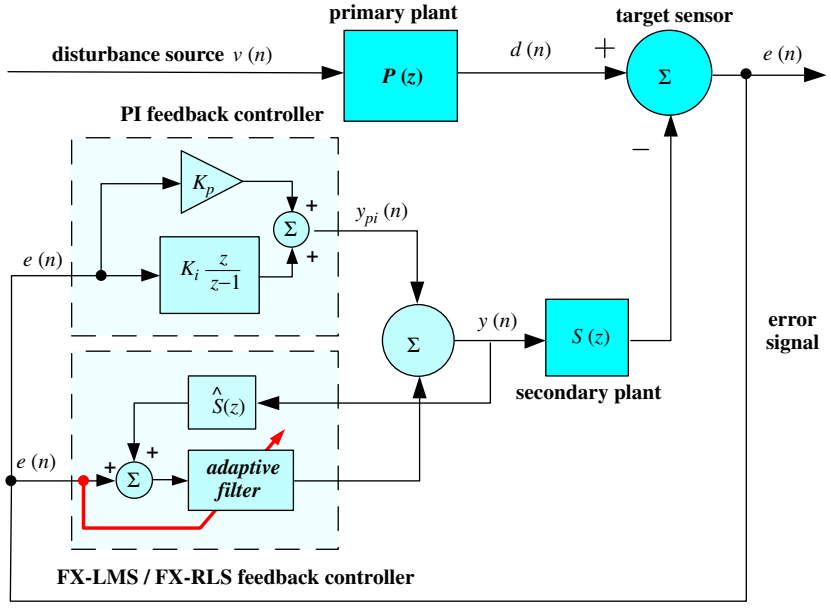

Fig. 7. Feedback adaptive filter with parallel PI controller.

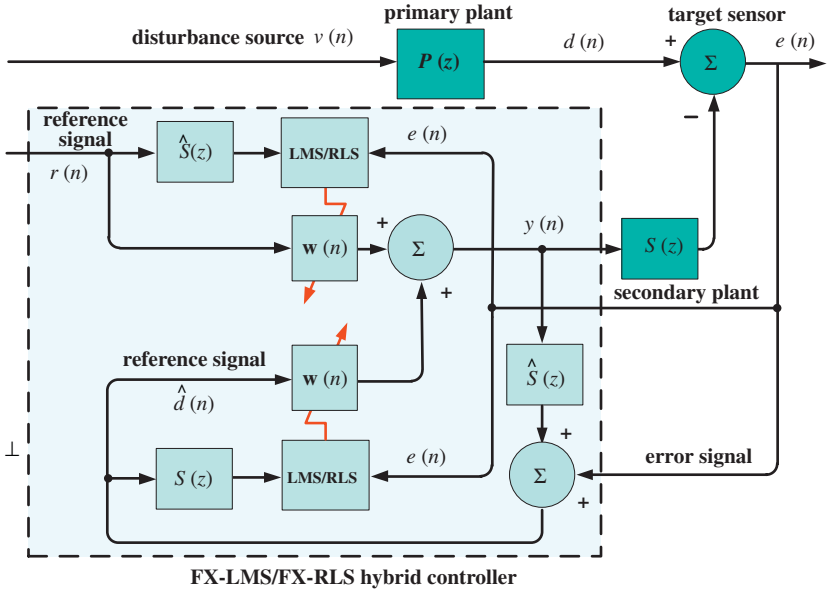

Fig. 8. Hybrid adaptive filter implementation (parallel PI controller not shown).

it works properly in experiments. A diagram of the hybrid adaptive filter is shown in Fig. 8.

6. Target tracking with adaptive filters

In the previous section, adaptive filter methods were proposed to point the beam at a static target, the (0,0) position on the target PSD. While these methods are directly applicable to many beam control applications, other beam control scenarios exist such that the target is dynamic. The adaptive filter algorithms developed in the previous section can be slightly modified to track a target by simply modifying the error signal definition from Eq. (2). The desired position is no longer the target center, but the tracking signal, say $d_t(n)$. Therefore, Eq. (2) is modified to include the tracking signal:

$$e(n) = d(n) - s(n) * y(n) - d_t(n) \tag{18}$$

Initial testing with the feedforward adaptive filter tracker showed instability with the dynamic target. The reason is guessed that the dynamics of the moving target is too fast relative to the adaptation rate of the feedforward adaptive filter. To compensate for this problem, the feedforward adaptive filters can be placed in parallel with a PI controller as done with feedback and hybrid configurations from the previous section.

7. Experiments and results

7.1. System identification

As mentioned previously, the developed control methods require a model of the secondary plant dynamics of the CFSM. It is required for the Filtered-X methods and for internally estimating the disturbance signal for the adaptive feedback filter control. Therefore, a system identification was conducted first to obtain its transfer function $\hat{S}(z)$ using MATLAB's System Identification toolbox. Experiments showed negligible coupling between the two axes of the CFSM. An input to one axis of the mirror yields less than 10% movement in the other axis for typical amplitude used in the experiments. Therefore, system identification is performed for each axis separately. Beerer (2008) contains more detailed explanation of the system identification methods used in this study.

7.2. Disturbance and reference signals

Several experiments with various scenarios were run on the testbed to explore the capabilities of the proposed control techniques. Table 2 summarizes the characteristics of the disturbances from different sources and their individual contributions to the beam position error at the target. The data is reported

Table 2
Jitter disturbance characteristics.

Target	Bias (DC)	Narrowband (Shakers)	Broadband (DFSM)	Total jitter
Off-board	≈ 1000 μm	40 Hz, $\sigma \approx 40$ μm 60 Hz, $\sigma \approx 30$ μm	0–200 Hz band-limited white noise, $\sigma \approx 51$ μm	$\sigma \approx 71$ μm
On-board	≈ 1000 μm	40 Hz, $\sigma \approx 18$ μm 60 Hz, $\sigma \approx 17$ μm	0–200 Hz band-limited white noise, $\sigma \approx 48$ μm	$\sigma \approx 52$ μm

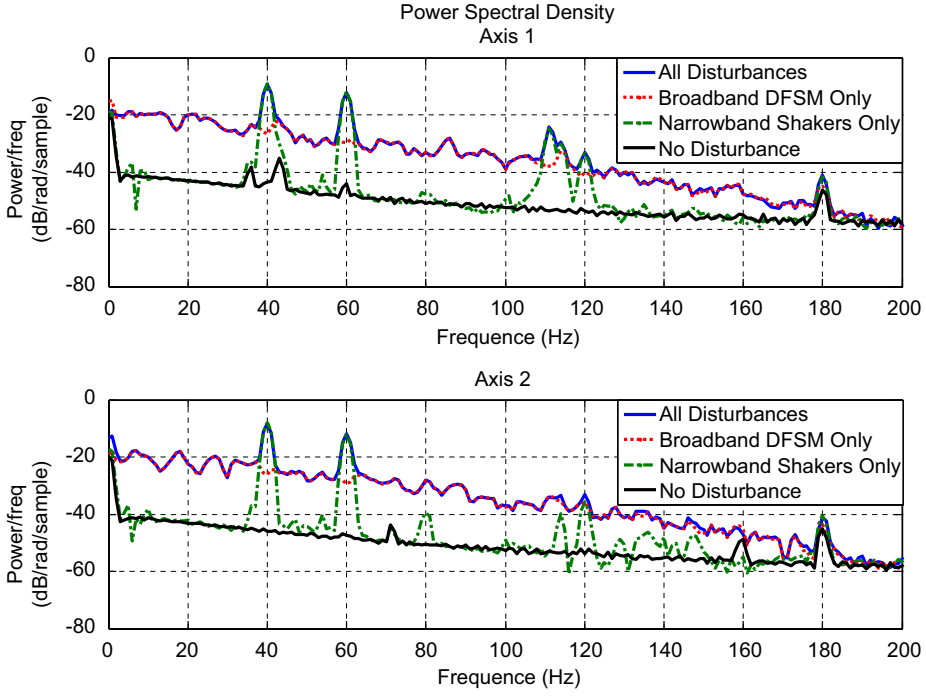

Fig. 9. PSD plot of beam jitter from combined and individual disturbance sources.

as the standard deviation, σ, of the jitter radius. Experiments were conducted with the target sensor in two different positions (on and off the vibration platform). The effects of the disturbances vary between the two target positions. The power spectral density plot (PSD) of the beam position at the off-board target in the presence of the disturbances is shown in Fig. 9. The individual contributions to the total beam jitter are shown by additionally plotting the DFSM and shaker disturbances separately. The shaker frequencies at 40 Hz and 60 Hz can be clearly seen.

In order to give more insight into the performance of the developed control laws, a series of experiments was conducted to characterize the degree of correlation between the various reference signals and the disturbances at the target. Using experimental data from the error and reference sensors with no control, the optimal Wiener jitter rejection index, γ_{opt} from Eq. (6), was calculated comparing each individual reference signal and disturbance source. The results in Table 3 represent the best possible performance for a given reference signal with a linear transversal filter with 45 taps. The target sensor (PD-2) was mounted in its off-board position, and the reference signals are filtered for the Filtered-X modification. For attenuating all disturbances, the off-board PSD reference signal will perform significantly better than the on-board PSD alone. Also, as expected, the accelerometer reference signals would be successful at rejecting the shaker disturbances but completely ineffective for control of the DFSM disturbance.

Due to the two orthogonally mounted shakers, the vibrational disturbance is complex and along all three axes of the platform. Choosing a proper signal from the 3-axis accelerometer to use as a reference is not arbitrary. For this research, the accelerometer signal that produced in best results in the optimal jitter rejection experiment from Table 3 was used. Therefore, the *Z*-axis accelerometer signal was used for both axes of the control law (Axis-1 and Axis-2). In a more complex system with many sources of vibration this technique may not be appropriate. In such a system the signals from all three axes of the accelerometer could be used in the control law.

7.3. Control parameters

In Bateman (2007), it was experimentally observed that when using a PSD reference signal, the FX-LMS controller performs its best with a single tap. This was confirmed in the present experiments again, however when using an accelerometer reference signal, the higher filter order had the greater performance. The LMS convergence factor was chosen, by trial and error, to be $\mu = 0.5$. All the following FX-LMS data was taken using a single tap for the PSD, 45 taps for the accelerometer ($M_p = 1, M_a = 45$). For the FX-RLS controller, the forgetting factor was chosen to be $\lambda = 0.99$. Multiple taps performed best for the PSD and accelerometer reference signals. The FX-RLS controller needed more accelerometer taps than PSD taps to effectively attenuate the jitter ($M_p = 10, M_a = 45$).

The feedback FX-LMS adaptive filter used a convergence factor of $\mu = 0.5$ and single tap, $M_{FB} = 1$. For the FX-RLS feedback controller, a forgetting factor of $\lambda = 0.99$ and $M_{FB} = 50$ taps was used. The hybrid adaptive filter used parallel feedback and multiple reference signal feedforward filters. The FX-LMS hybrid controller used a single feedback tap, a single feedforward on-board PSD tap and 30 feedforward accelerometer taps ($\mu = 0.5$, $M_{FB} = 1$, $M_p = 1$, $M_a = 30$). The FX-RLS hybrid controller used 10 feedback taps, 10 feedforward on-

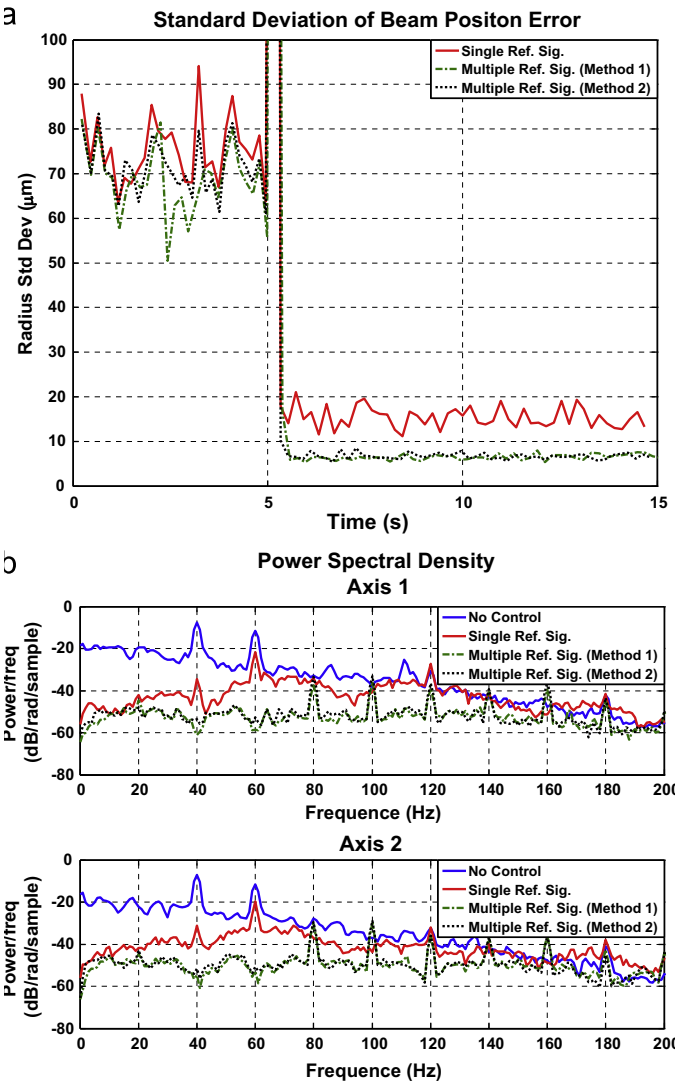

Fig. 10. Comparison with different reference signals (feedforward FX-RLS, off-board target): (a) standard deviation of beam position and (b) power spectral density of beam position.

Table 3
Optimal Wiener jitter rejection, γ_{opt} from Eq. (6) (Off-board target).

Disturbance source	Reference signal									
	Off-board PSD (coherent)		On-board PSD (semi-coherent)		Accel. *X*-axis		Accel. *Y*-axis		Accel. *Z*-axis	
	Target axis		Target axis		Target axis		Target axis		Target axis	
	1	2	1	2	1	2	1	2	1	2
DFSM	0.958	0.959	0.958	0.957	0.081	0.144	0.098	0.151	0.093	0.120
Shakers	0.951	0.944	0.636	0.889	0.553	0.663	0.875	0.853	0.951	0.933
All dist.	0.833	0.841	0.578	0.692	0.290	0.275	0.342	0.408	0.411	0.402

board PSD taps and 30 accelerometer taps ($\lambda = 0.99$, $M_{FB} = 10$, $M_p = 10$, $M_a = 30$).

A PI controller was placed in parallel with the feedback and hybrid adaptive filters. The PI control gains were tuned manually to $K_p = 0.05$ and $K_i = 200$.

7.4. Jitter rejection control: for stationary target

The first set of experiments is designed to evaluate the jitter rejection performance of the developed control methods. In these experiments, the control objective is to regulate the optical beam to the dead-center of the off-board target PSD with attenuating jitter. For each experiment, the testbed was run for a total of 15 s. The controller turns on after an elapsed time of 5 s and attempts to push the beam to the target center and remove the jitter. The standard deviation is calculated for the beam position (in μm) as a measure of the tightness or spread of the beam.

7.4.1. Single full-coherent vs. multiple semi-coherent reference signals

First, the multiple semi-coherent reference feedforward adaptive filters (which uses both on-board PSD and accelerometer signals) were compared to the single fully coherent filter (which uses the off-board PSD signal). The feedback filter loop and PI control loop are turned off.

Fig. 10 shows the standard deviation of beam position and its power spectral density with the feedforward FX-RLS filter. The performance of using either Method 1 or Method 2 for combining the reference signals in the control law was nearly identical. In terms of steady state jitter rejection, the feedforward adaptive filter controller performed significantly better with multiple semi-coherent reference signals than the fully coherent reference signal. (Using the performance index γ_{cont} defined in Eq. (7), the control performance for each axis can be expressed as (0.785, 0.799), (0.895,0.919), (0.895,0.921) with the single off-board PSD, the multiple reference signals using Method 1 and Method 2, respectively.) These findings should be expected because of the complex nature of the disturbances. In the present testbed setup, disturbances are generated by two distinct sources and disturb beam positions measured in the target PSD (PD-2) and the off-board reference PSD (PD-1). So the reference signal measured at the off-board reference PSD is correlated to these two distinct disturbances. However, the distinct disturbances may yield effects on PD-1 and PD-2 in a different manner: for instance, the disturbance from DFSM may be more potent than that of shakers in PD-2, while the contrary may happens in PD-1.

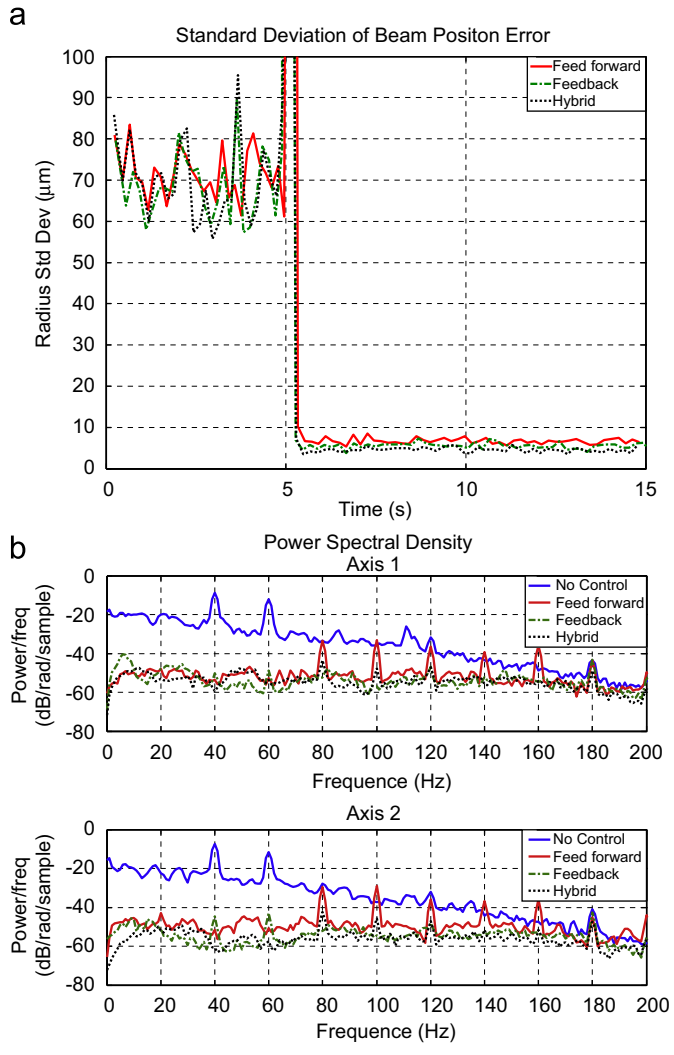

Fig. 11. Comparison with different structures (FX-RLS, off-board target): (a) standard deviation of beam position and (b) power spectral density of beam position.

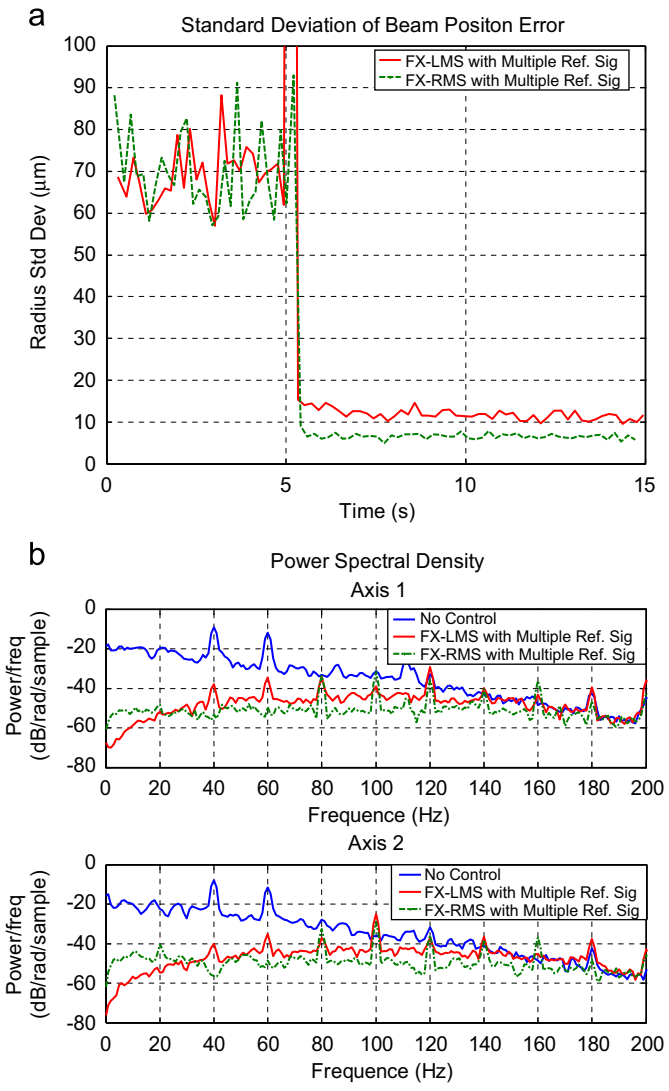

Fig. 12. Comparison of adaptive algorithms (FX-LMS vs. FX-RLS): (a) standard deviation of beam position and (b) power spectral density of beam position.

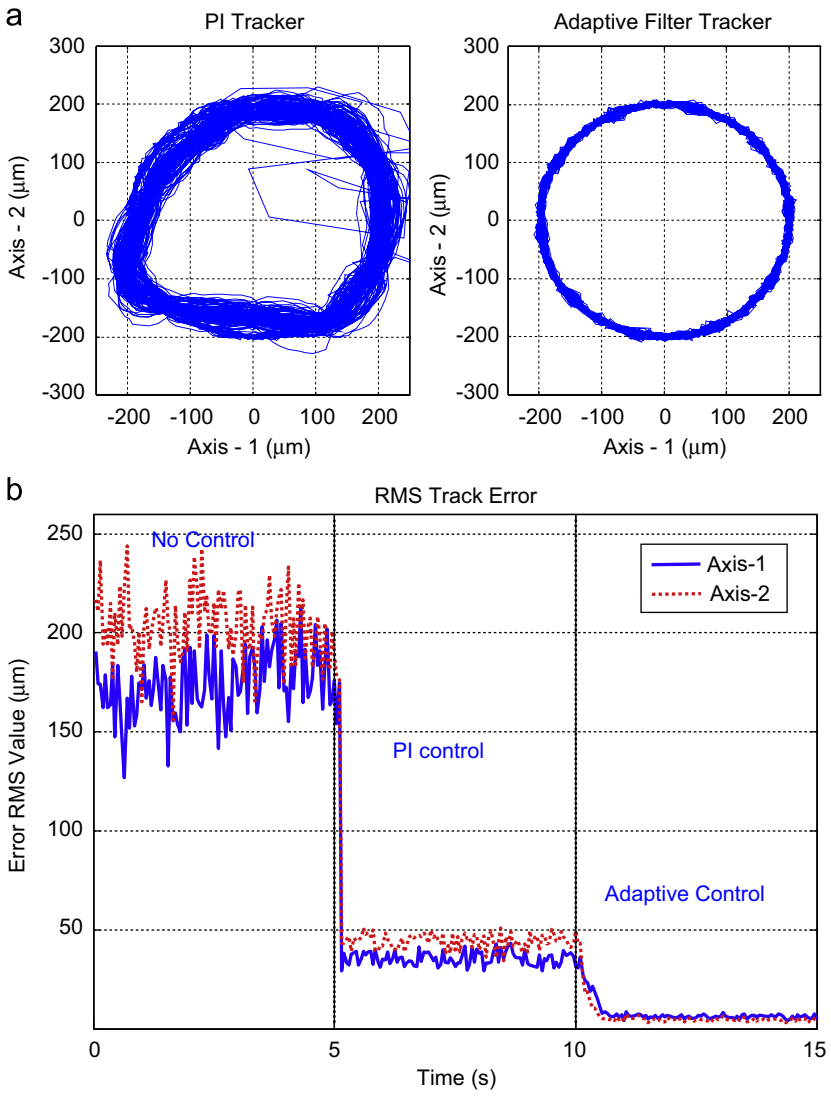

Fig. 13. Tracking performance (PI control vs. FX-RLS hybrid control): (a) beam trace plot and (b) RMS tracking error.

On the other hand, reference signals from the on-board PSD and the accelerometer are separately correlated to the distinct disturbances and thus their combination may provide more information to the controller than the single off-board PSD reference.

7.4.2. *Feedforward vs. feedback vs. hybrid filters*

This section compares the developed feedback and hybrid adaptive filters with the best performing feedforward technique (using multiple reference signals). As previously mentioned, feedback adaptive filter control has the great advantage of not requiring any measured reference signal. Moreover, the reference signal in Eq. (16) is an estimate of the combined effect $d(n)$ of the different disturbing sources on the system output, so it may be more correlated with errors at the target PSD than any other measured reference signals, provided the model $\hat{S}(z)$ is close enough to the actual system $S(z)$.

Fig. 11 shows the results of the FX-RLS experiment. In the present experiment, the feedback technique had better overall steady state jitter rejection and convergence times than feedforward control, and the hybrid technique produced even better results than feedback alone, but the differences are not significant. (The performance index γ_{cont} for each axis is (0.895,0.921), (0.928,0.917), (0.935,0.931) with feedforward, feedback, and hybrid controllers, respectively.)

7.4.3. *FX-LMS vs. FX-RLS*

At the price of being more computationally expensive the FX-RLS algorithm performs better than FX-LMS at attenuating the optical beam jitter. Fig. 12 shows a comparison of the two controllers. Both algorithms are successful at attenuating broadband disturbances. However, the FX-RLS controller far exceeds the FX-LMS at canceling the narrowband disturbances caused by the shakers.

7.5. *Target tracking*

In this experiment, the adaptive filter controllers were asked to track a small circle on the target PSD while being subjected to the same narrow and broadband disturbances as in Section 7.4. The beam tracks a 200 μm radius (or approximately 160 microradian half-angle) circle on the detector at a rate of 20 Hz. The experiments were conducted with the target sensor in the off-board position only. This configuration imitates actual target tracking applications. Each experiment is run for 15 s, 0–5 s is open-loop (or no control). The PI controller turns on at $t=5$ s; and

at $t=10$ s, the adaptive filter controller turns on and runs in parallel with the PI controller.

Fig. 13 shows the RMS track error plot and a beam trace plot comparing the PI tracker to the FX-RLS hybrid tracker, respectively. The figures dramatically demonstrates the improvement of performance achieved by using the adaptive filter tracker. Not only does the PI controller trace a different path at each revolution, but also the mean path is not circular. The adaptive filter tracker closely traces the 200 μm circle.

8. Contribution and conclusion

The contributions of this work are presenting adaptive control methods which are effective and easy to implement in practical applications and verifying them in a testbed which simulates more realistic situations. The developed methods use adaptive filters with the simplest filter structure (the transversal filter) and the classical PI controller, so they are much easier to understand and implement than the previous works, but showed equivalent jitter control performance. The use of multiple semi-coherent reference signals is not only more practically feasible but also provides more information to the controller than the off-board PSD signal and thus show better jitter rejection performance. An index variable is presented to measure how 'good' the reference signal is. Based on its value, one can choose the right reference signals among many available signals considering trade-off between performance and complexity of the jitter rejection control.

The two feedforward methods developed for combining the reference signals in the controller showed near identical performance. The feedback adaptive method is also presented and performed even better than any feedforward technique, but it requires a highly accurate actuator model and another LTI control block in parallel. The hybrid control, combining the feedback and feedforward filters, performed still better and showed higher than 90% jitter attenuation for combined narrowband/broadband disturbances in the experiment.

Adaptive filter methods were successfully demonstrated for tracking a dynamic target as well. The hybrid controller had greater performance than a classical PI target tracker. In many cases, instability was an issue with the adaptive filters, especially when a large DC bias was attempted to be rejected and/or the target is dynamic. To increase the stability and overall robustness of the controller, a classical PI controller should be used in parallel with the adaptive filters.

The developed controllers are single-input–single-output or single channel in adaptive filter terms. The use of multi-input–multi-output or multi-channel adaptive filters could couple the control between the axes of the CFSM and could possibly further improve performance, and the authors suggest this topic for future study.

References

Anderson, E., Blankinship, R., Fowler, L., Glaese, R., & Janzen, P. (2007). Adaptive filtering and feed-forward control for suppression of vibration and jitter. In *Proceedings of SPIE* (Vol. 6569, 65690Q), Orlando, FL.

Bateman, B. E. (2007). *Experiments on laser beam jitter control with applications to a shipboard free electron laser*. Master's Thesis. Monterey, CA: Naval Postgraduate School.

Beerer, M. J. (2008). *Adaptive filter techniques for optical beam jitter control and target tracking*. Master's Thesis. Monterey, CA: U.S. Naval Postgraduate School.

Haykin, S. (2000). *Adaptive filter theory* (4th ed.). New Jersey: Prentice Hall.

Jiang, S.-B., & Gibson, J. S. (1995). An unwindowed multichannel lattice filter with orthogonal channels. *IEEE Transactions on Signal Processing*, *43*, 2831–2842.

Kuo, S. M., & Morgan, D. R. (1996). *Active noise control systems: Algorithms and DSP implementations*. New York: Wiley-Interscience.

McEver, M. A., Cole, D. G., & Clark, R. L. (2004). Adaptive feedback control of optical jitter using *q*-parameterization. *Optical Engineering*, *43*, 904–910.

Orzechowski, P. K., Chen, N., Gibson, S., & Tsao, T.-C. (2006). Optimal jitter rejection in laser beam steering with variable-order adaptive control. In *Proceedings of the 45th IEEE conference on decision and control* (pp. 2057–2062), San Diego, CA.

Orzechowski, P. K., Gibson, J. S., & Tsao, T.-C. (2004). Optimal disturbance rejection by lti feedback control in a laser beam steering system. In *Proceedings of the 43th IEEE conference on decision and control* (pp. 2143–2148), Atlantis, Paradise Island, Bahamas.

Pérez Arancibia, N. O., Chen, N., Gibson, S., & Tsao, T.-C. (2006). Adaptive control of jitter in laser beam pointing and tracking. In *Proceedings of SPIE* (Vol. 6304, 63041G, pp. 63041G.1–63041G.12).

Pérez Arancibia, N. O., Chen, N. Y., Gibson, J. S., & Tsao, T.-C. (2006). Variable-order adaptive control of a microelectromechanical steering mirror for suppression of laser beam jitter. *Optical Engineering*, *45*.

Watkins, R. J. (2004). *The adaptive control of optical beam jitter*. Ph.D. Thesis. Monterey, CA: U.S. Naval Postgraduate School.

Watkins, R. J., & Agrawal, B. N. (2007). Use of least means squares filter in control of optical beam jitter. *Journal of Guidance, Control, and Dynamics*, *30*, 1116–1122.

Yoon, H., Bateman, B., & Agrawal, B. (2008). Laser beam jitter control using recursive-least-square adaptive filters. In 2008 *directed energy systems symposium*, *beam control conference proceedings*. Monterey, CA: Directed Energy Professional Society.

Yoon, H., Bateman, B., & Agrawal, B. (2011). Laser beam jitter control using recursive-least-squares adaptive filters. *ASME Journal of Dynamic Systems, Measurement and Control*, *133* 041001-1–041001-8.